

# Application of Sliding Fuzzy Control on Robust Algorithm for Frequency Estimation of Distorted Signals in Power Systems

KUO-NAN YU      CHENG-MING LEE\*

Department of Electrical Engineering  
National Chin-Yi University of Technology  
35, Lane 215, Sec. 1, Chungshan Road, Taiping, Taichung, Taiwan  
yukn@ncut.edu.tw

\*Department of Computer and Communication Engineering  
Nan Kai University of Technology  
Tsaotun, Nantou 542, Taiwan  
t104@nkut.edu.tw

*Abstract*—This paper presents a sliding fuzzy control (SFC) to adapt the exponent of robust algorithm to a signal with a variable frequency in a power system. With the aid of SFC, the robust algorithm can more improve the performance of extended complex Kalman filter (ECKF) at the severe variation of frequency. The proposed method is involved in ECKF's algorithm without changing any form; besides, it can enhance the estimation accuracy and reduce the computation time. Results of comparative studies of the technique proposed with the ECKF with robust algorithm (RECKF) and RECKF-SFC are presented in the paper.

*Key-Words:* - Kalman Filter, Robust Algorithm, Sliding Fuzzy Controller, Frequency Estimation, Distorted Signals.

## 1 Introduction

Frequency estimation plays an important role in a power system since the variation in system frequency is generally used to indicate the system operation state. For example, if the frequency is beyond the limitation, a mismatch between generation and load may occur. Furthermore, the frequency can be used as a base for estimating other parameters including the amplitude and phase of voltage signals. Thus, reliable frequency estimation is necessary for many applications in a power system such as effective power control, setting of protective relays for load shedding and restoration, power quality monitoring, and generation protection.

Traditionally, the frequency is estimated by the time between two zero crossings as well as the calculation of the number of cycles [1], [2]. However, this method is relatively sensitive for distorted signals. To improve this drawback, many methods had been proposed such as discrete Fourier transforms [3], transforming discrete Fourier transforms [4], Prony's estimation [5]. Nevertheless, these algorithms suffer from inaccuracies due to more violent fluctuations in the measured signal.

Moreover, the high-order terms in the Taylor's expansion for methods including least square error technique [6], [7], Kalman filtering [8]-[10], adaptive notch filters, multiple frequency tracker [11], recursive Newton-type algorithm [12], [13], orthogonal components filtered algorithm [14], [15], and a new variant of the extended Kalman filter [16] were neglected to optimize estimations due to the presence of nonlinear functions in the formulation of measurements. However, frequency estimation of distorted signals using these methods may occur incorrectly or take longer time to converge and even diverge.

Recently, [17]-[20] have shown the extended Kalman filter for frequency estimation of polluted signals with higher noise to make the measurement function as the likelihood of linear formulation in order to reduce the influence of high-order terms. However, it still cannot accurately track the frequency in the presence of abnormal values of measurements due to harmonics and disturbances. Generally, the extended Kalman filter (EKF) applied to estimate frequency of signals may have undesirable properties which are described as follows:

- (1) It requires good knowledge of state equation and measurement equation to obtain a proper estimation, especially for both equations containing zero-mean white noise. If the theoretical behavior of the EKF and its actual behavior do not agree, divergence problems will occur.
- (2) It exists the model uncertainties which cannot be expressed by the linear state-space model since an actual system is nonlinear. Thus, using the linear state-space model to represent an actual system may increase modeling errors.
- (3) It can accurately estimate the amplitude variation when the fundamental frequency is fixed. However, it cannot automatically return itself to the new incoming frequency in which the frequency changing.
- (4) It often suffers from divergence problems for harmonic state estimation caused by the dropping off effect.
- (5) The nonlinearity has often caused the EKF to diverge in some poorly initial conditions when the EKF is applied to the problem of estimating the parameters of a multiharmonic signal in white noise, where the system dynamics is linear, but the observation of the state is nonlinear.

Since the main drawback of the EKF is its computational expense, the extended complex Kalman filter (ECKF) has further been proposed with the aid of the hysteresis band to speed up the convergence. Nevertheless, the ECKF has to handle two problems as it is applied on an actual practical signal. One is it cannot properly track the variations if the signal varies drastically. This is because the choice of hysteresis band only considers the noise. The other is the band choice is depended upon the expert's experience which is inconvenient for applying to different power systems. Although [21] and [22] had used self-tuning to update the covariance of the ECKF for better performances, they need more executing time in iterations of updating which is not suitable for a practical system.

In [23], [24], a robust algorithm incorporated in ECKF is presented for frequency estimation of distorted signals in a power system. It formulates the absolute residual vector as the weighting function such that the abnormal condition can take it into account. If the absolute residual vector is increased, it can then be inversed to suppress the influence in order to obtain better estimations. Conversely, if it is considerably small, it will, at most, be equal to one. Thus, this weighting function will not affect estimations. However, this weighting function only senses abnormal measurement due to harmonic and bad measurement, but it can't know the power

signal's severe variation like sudden load change. In [25] a sliding fuzzy controller embedded into the ECKF to compensate the prediction results. The concept of the sliding mode control combines the residual and the change-in-residual as an integrated input variable. Hence, the number of fuzzy rules can be largely reduced to facilitate the computation performance. In this paper, the sliding fuzzy controller is taken as the estimator to estimate a tuningable term for increasing the performance of weighting function at signal's severe variation.

## 2 The Proposed Approach

Fig.1 shows a block diagram of the proposed method in this paper. As seen from Fig.1, a sliding fuzzy controller (SFC) is added to adjust the exponent of robust algorithm to enhance the performance of ECKF at signal's severe variation.

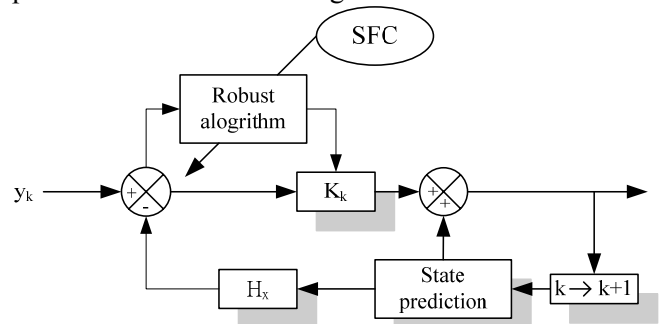


Fig.1 Block diagram of the proposed method

### 2.1 Signal Model

In a power system, an observed signal  $y_k$  at time point  $k$  is a sum of  $z_k$  of  $M$  sinusoids with white noise  $v_k$  as written to be

$$y_k = z_k + v_k \quad k = 1, \dots, N$$

$$v_k \sim N(0, R_k) \tag{1}$$

where

$$z_k = \sum_{n=1}^M a_n \sin(\omega_n t_k + \phi_n), \quad M = 1, 2, 3, \dots$$

$$\omega_n = 2\pi f_n$$

$$t_k = kT_s, \quad T_s \text{ is the sampling time.} \tag{2}$$

In (2), parameters  $a_n$  and  $f_n$  are the amplitude with initial phase  $\phi_n$  and the frequency of the  $n$ th sinusoid, respectively. The observation noise  $v_k$  is a Gaussian white noise with zero-mean and variance  $\sigma_v^2$ . The measurement error covariance is  $R_k = E[v_k v_k^{*T}]$ , where \* means the complex conjugate and T is the transpose.

For notice of the fundamental frequency, let us consider a single sinusoid  $z_k$  with angular frequency

$\omega_1$  in the presence of white noise under the assumption that the number  $M$  of sinusoids is known ( $M = 1$ ). For this reason, the signal in (2) can be simplified to be

$$z_k = a_1 \sin(k\omega_1 T_s + \phi_1) \quad (3)$$

where

- $\omega_1$  fundamental of angular frequency
- $\phi_1$  fundamental of phase angle
- $a_1$  fundamental amplitude of the signal

Note that the amplitude  $a_1$  and the variance  $\sigma_v^2$  are unknown [17].

Next, let us describe complex types of state variables used in this paper. Using a complex type to represent the state variable  $x_k$  of a time-varying single sinusoid signal is defined as follows:

$$x_{k(1)} = e^{j\omega_1 T_s} \quad (4)$$

$$x_{k(2)} = a_1 e^{j(k\omega_1 T_s + \phi_1)} \quad (5)$$

$$x_{k(3)} = a_1 e^{-j(k\omega_1 T_s + \phi_1)} \quad (6)$$

The measured value of the signal can then be written to be

$$\text{State equation } x_k = f(x_{k-1}) \quad (7)$$

$$\text{Measurement equation } y_k = Hx_k + v_k \quad (8)$$

where

$$x_k = [x_{k(1)} \ x_{k(2)} \ x_{k(3)}]^T \quad (9)$$

$$f(x_{k-1}) = \begin{bmatrix} x_{k-1(1)} & x_{k-1(1)}x_{k-1(2)} & \frac{x_{k-1(3)}}{x_{k-1(1)}} \end{bmatrix}^T \quad (10)$$

$$\text{Measurement matrix } H = [0 \ -0.5i \ 0.5i] \quad (11)$$

## 2.2 ECKF for Frequency Estimation

The ECKF is an optimal dynamic estimator and is suitable for describing state variables in a power system. The ECKF process is divided into state prediction and state filter as shown in Fig.1. The former performs prediction processing with reference to the history data and the latter is to find the optimal estimate considering all available measurements and predicted states. The recursion process of the ECKF through linearization for estimating the signal parameters of sinusoid waves is described as below:

*State prediction:*

$$\tilde{x}_k = f(\hat{x}_{k-1}) \quad (12)$$

and the predicted error covariance  $M_k$  is

$$M_k = F_k P_{k-1} F_k^{*T} + Q_k \quad (13)$$

where

$$F_k = \frac{\partial f(\hat{x}_{k-1})}{\partial \hat{x}_{k-1}} = \begin{bmatrix} 1 & 0 & 0 \\ \hat{x}_{k-1(2)} & \hat{x}_{k-1(1)} & 0 \\ -\hat{x}_{k-1(3)}/\hat{x}_{k-1(1)}^2 & 0 & 1/\hat{x}_{k-1(1)} \end{bmatrix} \quad (14)$$

In (12), the symbols  $\sim$  and  $\hat{\cdot}$  stand for the predicted and estimated values, respectively.

*State filter:*

$$\hat{x}_k = \tilde{x}_k + K_k (y_k - H\tilde{x}_k) \quad (15)$$

The Kalman gain  $K_k$  is calculated to be

$$K_k = M_k H^{*T} [H M_k H^{*T} + R_k]^{-1} \quad (16)$$

and the parameter  $R_k$  in (16) is generally set to be equal to one. Moreover, the filtered error covariance  $P_k$  for updating the estimation is written to be

$$P_k = M_k - K_k H M_k \quad (17)$$

where

- $\hat{x}_k$  state variable after estimation
- $\tilde{x}_k$  state variable after prediction
- $K_k$  Kalman gain
- $y_k - H\tilde{x}_k$  innovation vector

In conclusion, the state prediction is used to calculate the value at time point  $k+1$  based on the estimated value at time point  $k$ . If signals have been changed greatly at time point  $k$ , the estimator will not be able to follow this situation and to provide proper weighting. As a result, it will not be able to predict a value which is close to the real value at time point  $k + 1$ . Nevertheless, if a normal operation algorithm is still used for predicting a value, the innovation vector will change unusually and the gain will amplify the unusual change that reduces filter results. Moreover, the initial values of the state variable  $\hat{x}_0$ , covariance  $P_0$ , and error covariance  $R_0$  are related to the speed of convergence. Those values are generally set to be equal to one. Based on the recursive process to reset the covariance, the algorithm of the Kalman filter can be used to track the change of parameters of voltage

signals. The parameters of frequency  $\hat{f}_{(k)}$ , amplitude  $\hat{a}_{(k)}$ , and phase angle  $\hat{\phi}_{(k)}$  at time point  $k$  can then be optimally estimated by applying the state variables to the ECKF as expressed to be

$$\hat{f}_{(k)} = \frac{1}{2\pi T_s} [\text{Im}(\ln(\hat{x}_{k(1)}))] \quad (18)$$

$$\hat{a}_{(k)} = |\hat{x}_{k(2)}| \quad (19)$$

$$\hat{\phi}_{(k)} = \text{Im} \left[ \ln \left( \frac{\hat{x}_{k(2)}}{|\hat{x}_{k(2)}| \times (\hat{x}_{k(1)})^k} \right) \right] \quad (20)$$

where the abbreviation Im stands for the imaginary part of a quantity.

### 2.3 RECKF for Frequency Estimation

Under normal operating conditions, the ECKF is an optimal dynamic estimator which is suitable for describing state variables in power systems. However, the accuracy of frequency estimation using the ECKF may be affected by power system disturbances. Thus, a robust ECKF (RECKF) is proposed by applying the exponential function to limit the variation of the innovation vector, to restrain the unusual measured value, and to enhance the estimated accuracy. The detail of this algorithm is described as follows.

The measurement error covariance  $R_k$  is the inverse of the weighting  $W_k$  as written to be

$$R_k = W_k^{-1} \quad (21)$$

$$W_k = W_{k-1} \exp(-|y_k - H\tilde{x}_k|) \quad (22)$$

where the exponential term  $\exp(-|y_k - H\tilde{x}_k|)$  is the absolute residual vector. Moreover, the variable  $R_k$  is used to substitute into (16) and to control the Kalman gain of the ECKF as well as restrain inaccurately measured values or unusual changes of parameters. When some measured values occur unusually, the measured value of time-varying signals  $y_k$  will change a lot. However, the prediction of state variables  $\tilde{x}$  does not yet detect the unusual measured value at this point. As a result, the computation of  $H\tilde{x}_k$  is still in a normal state that can add the absolute value of the innovation vector. In other words, when the measured value is distorted, the absolute value of the innovation vector will increase, and the value of the robust exponential function will then decrease. Consequently, it can assist in reducing the weighting and mitigating the error. In addition,

since the RECKF can adjust the weighting of the Kalman gain  $K_k$  at each estimated time step according to the change of signals, it is therefore more efficient. On the other hand, the ECKF cannot distinguish the great change from the measured value because the weightings are all the same throughout the estimated process. This means the ECKF will take more time to converge. Thus, estimation using the ECKF will be less effective than the RECKF.

### 2.4 Sliding Fuzzy Controller

Basically, the sliding surface-enhanced fuzzy adaptive controller uses the residual and change-in-residual as inputs and computes a criterion with fuzzy rules to adapt the signal's variation. Due to including the residual and change-in-residual, the decision of the proposed method can handle more the severe variation. Furthermore, the proposed method produces a criterion automatically so it can be convenient to use in different power systems. As a result, the proposed method is adequate to apply to real signal of power systems. To speed up computing in fuzzy rules for real-time and on-line operation, two inputs of this sliding fuzzy controller are combined into one to reduce the number of fuzzy rules; that is, only one variable is used in the antecedents of the fuzzy rules for participating in decision making process. The computation steps of the fuzzy adaptive controller are described as follows.

#### *Step 1. Choice of Input and Output Variables:*

As the residual  $r_k$  and change-in-residual  $\dot{r}_k$  are combined into an integrated input variable of the fuzzy control system, an output variable can then be obtained by the fuzzy controller. In this study, the input variable  $g$  is similar to the expression of the sliding surface in a second-order system [26] and is defined by

$$g = |\lambda r_k + \dot{r}_k| \quad (23)$$

where  $\lambda$  is the positive constant and the residual  $r_k$  is computed as below

$$r_k = y_k - H\tilde{x}_k \quad (24)$$

where  $y_k$  and  $H\tilde{x}_k$  individually indicates the measured and predicted value at time point  $k$ . The change-in-residual  $\dot{r}_k$  at time point  $k$  can be also expressed to be

$$\dot{r}_k = \frac{r_k - r_{k-1}}{k - (k-1)} = r_k - r_{k-1} \tag{25}$$

Similarly, for the output variable represented by the symbol,  $\alpha^{crisp}$ , this fuzzy controller can be developed. Note that in this fuzzy adaptive controller, the variable  $g$  is assumed to be element of input vector  $G$ , and  $\alpha^{crisp}$  is assumed that of output vector  $U$ . As for the region of the universe of discourse of  $g$  and  $\alpha^{crisp}$ , the interval of  $g$  is assigned to be  $[-1.5, 1.5]$  and the interval of  $\alpha^{crisp}$  is assigned to be  $[0.2, 0.6]$ . These values have considered feasible based on the discussions with utility (i.e., Taiwan Power Company, TPC) engineers.

**Step 2. Fuzzy Rule Definition:** Let  $\bar{g}$  and  $\bar{\alpha}$  to be the linguistic variables for  $g$  and  $\alpha^{crisp}$ , respectively. Then, the universe of discourse is ready to partition in this step. Table 1 lists the input and output universes of discourses as well as the related fuzzy rules.

TABLE 1  
FUZZY SETS AND FUZZY RULES

Term set of linguistic variable	Label of fuzzy set				
$\zeta(\bar{g})$	$A_1$	$A_2$	$A_3$	$A_4$	$A_5$
$\zeta(\bar{\alpha})$	$C_1$	$C_2$	$C_3$	$C_4$	$C_5$

Fuzzy rules : IF  $\bar{g}$  is  $A_i$  THEN  $\bar{\alpha}$  is  $C_j$   
where  $i=1, \dots, 5$ , similarly for  $j$ .

**Step 3. Fuzzification:** In this step, the input variables in the fuzzy controller are mapped into a set of membership functions. The isosceles triangle is selected as the shape of the membership function. Moreover, the process of converting a crisp input value to a fuzzy value is based on a collection of logic rules in the form of IF-THEN statements.

**Step 4. Fuzzy Inference:** In this process, the max-min inference method is adapted [27]. If an input variable  $g$  with a linguistic value  $A_i$  defined by the universe of discourse  $G$  is given, its associated membership function is named as  $\mu_{ante}$ . The grade of membership of the antecedent  $\mu_{ante}$  is then formulated as below

$$\mu_{ante}(s) = \mu_{A_i}(g) \tag{26}$$

In (26), the variable  $s$  represents the number of linguistic terms in all of the antecedent terms. Note that there are a total of five fuzzy rules in the system as shown in Table 1 and no more than two rules will be used at the same time. Therefore, the inference result  $\mu_s(\alpha)$  obtained from the grade of membership of the consequent can be obtained to be

$$\mu_s(\alpha) = \text{Min}[\mu_{ante}(s), \mu_{C_j}(\alpha)] \tag{27}$$

**Step 5. Defuzzification:** In this process, the inference result for each input variable must be converted to a output value  $\alpha$ . Based on the center average defuzzification, the crisp output value can be computed to be

$$\alpha = \frac{\sum b_s \mu_s(\alpha)}{\sum \mu_s(\alpha)} \tag{28}$$

where  $b_s$  denotes the center of the membership function of the consequent of rule  $s$ .

**Step 6: Adjustment of exponent of robust algorithm:** The robust algorithm can be  $\exp(-\alpha|y_k - H\tilde{x}_k|)$ . However, once the system encounters large load changes, for example, the exponent will be adjust to adapt the severe variation.

Fig.2 shows the flowchart of the proposed approach. As seen from Fig.2, the weighting  $W_k$  and the sliding fuzzy controller are used to adjust the Kalman gain between state prediction and state filter. When the estimated system is operated in normal conditions, the value of the weighting  $W_k$  is close to 1, which means it does not need to tune its exponent. Meanwhile, the fuzzy adaptive controller will not reset the covariance. However, once the estimated system encounters abnormal conditions such as measurement errors or large load changes which result in a significant increment of the residual, the weighting  $W_k$  is then used to help on tuning the exponent. In addition, the sliding fuzzy adaptive controller can be used to help on tuning the Kalman gain. The aim of regulating the Kalman gain is to ensure the adaptability of the proposed approach on different conditions.

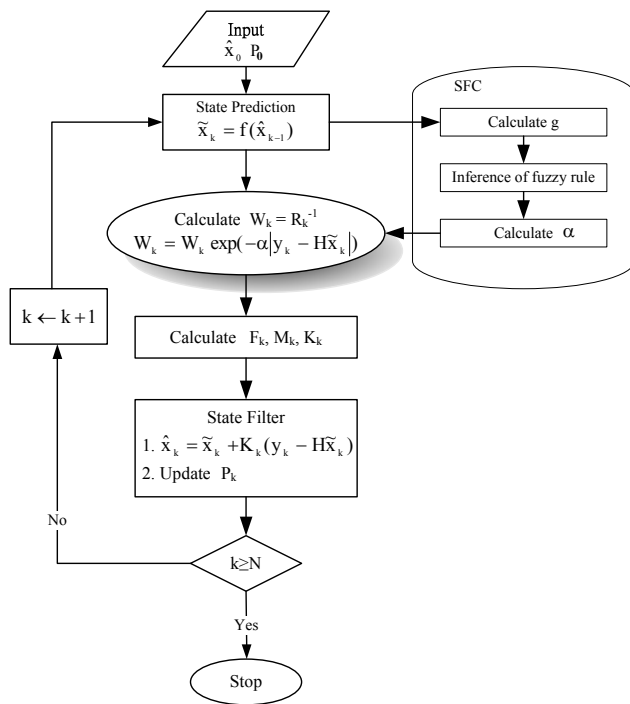


Fig.2 Flowchart of the proposed approach

### 3 Simulation Results

The proposed approach is verified with three cases and the obtained results are compared with those of the ECKF method. The initial values in the start point for state estimation were assumed as follows [18], [22]: For convenience, the initial state variables  $x_0$  were chosen to be 1.0, the filtered error covariance matrix  $P_0$  was selected to be diagonal with the value of 10 p.u.<sup>2</sup>. This means that one does not trust the initial state variables. The measurement error covariance matrix  $R_0$  was selected to be 1.0 p.u.<sup>2</sup> to represent an inaccurate measurement, and the model error covariance matrix  $Q_0$  is fixed to be 0.01 p.u.<sup>2</sup> in order to be realistic. Note that the covariance matrixes  $P_0$  and  $R_0$  will be updated during the estimation process of the proposed method.

#### Case 1: single change:

A signal with two cases is tested to verify the proposed method. Two conditions include the signal frequency and amplitude drops suddenly. The test signal consists of the fundamental frequency with white noise as follows:

$$\text{Test signal} = V_m \sin(k \omega T_s + \phi) + \text{white noise.}$$

Note that the amplitudes of test signals are set to be 1.0 p.u. and the sampling frequency is selected to be 10 kHz. Moreover, they contain Gaussian white noise with zero-mean and a standard deviation of 0.01 p.u. Generally, the frequency change in the system of TPC is limited to be  $\pm 0.5$  Hz. Thus, the measured frequency by the estimated filter will not be allowed beyond the band of 59.5 ~ 60.5 Hz.

**Condition 1: Frequency Drops Suddenly:** In this case, the frequency of the test signal is assumed to suddenly drop from 60 to 59.5 Hz at 0.1 seconds as the amplitude and phase angle are unchanged. The results of frequency and amplitude estimations using the ECKF and RECKF-SFC methods for the test signal are shown in Figs. 3 and 4, respectively. In those figures, the large variation is due to initial tracking so it doesn't need to care the performance of estimation. In the Fig.3, the estimated frequencies using the ECKF and RECKF-SFC have overshootings of 130.8 Hz and 88.9 Hz due to the variation of frequency, respectively. However, the proposed method (RECKF-SFC) has a less overshooting of 41.9 Hz. As seen from Figs. 4(a) and 4(b), the overshooting in the amplitude for the ECKF is 1.66 p.u., and the overshooting for the RECKF-SFC is 1.18 p.u. From those results, it can be found that the overshooting of the estimated frequency and amplitude is largely depressed by the RECKF-SFC. Thus, the proposed method is surely effective than the ECKF in the frequency and amplitude estimations.

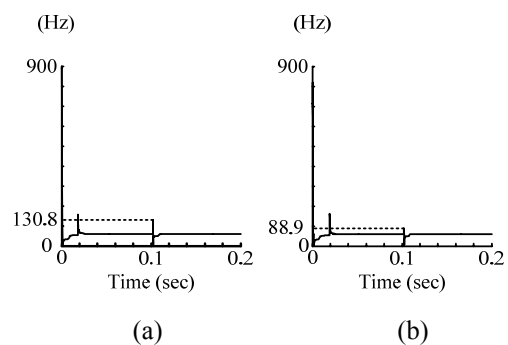


Fig.3 Frequency estimation (a) The ECKF method (b) The proposed method

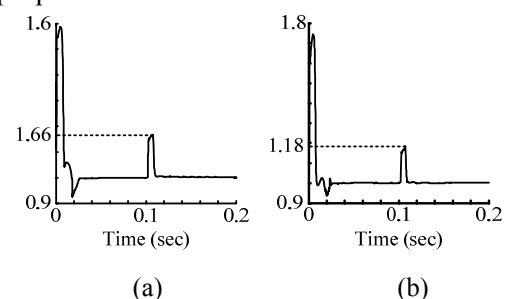


Fig.4 Amplitude estimation (a) The ECKF method (b) The proposed method

**Condition 2: Amplitude Drops Suddenly:** In this condition, the amplitude drops from 1.0 to 0.8 p.u. at 0.1 seconds, and the frequency and phase angle are unchanged. The results of frequency and amplitude estimations using the ECKF and RECKF-SFC for the first test signal are shown in Fig.5 and Fig.6. As seen from Fig.5, frequency and amplitude estimations using the RECKF-SFC have better results than the ECKF. In estimation of amplitude, the overshooting for ECKF is 0.78 p.u., and the ECKF-SFC can be 0.78. In estimation of frequency, the overshooting for ECKF is 82.82, and the result of proposed method is less 3.4 Hz due to SFC.

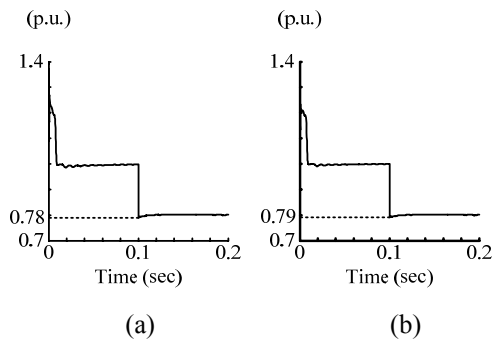


Fig.5 Amplitude estimation (a) The ECKF method (b) The proposed method

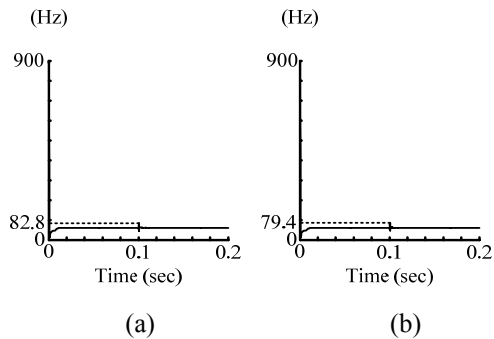


Fig.6 Frequency estimation (a) The ECKF method (b) The proposed method

**Condition 3: Frequency and Amplitude Simultaneously Change:** In this condition, the frequency and amplitude of test signals as shown in Fig.7 is assumed to simultaneously change from 60 to 59.5 Hz and from 1.0 to 0.8 p.u. at 0.2 s, respectively. The results of frequency and amplitude estimations using the ECKF and the proposed method for the test signal are shown in Figs. 8 and 9. As seen from Fig.8, frequency estimation using the proposed method has better result than those of the ECKF method.

Similarly, as seen from Fig 9, amplitude estimation using the proposed method also has better result than those of the ECKF method.

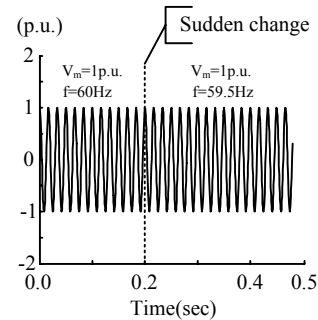


Fig.7 Test signals with condition 3

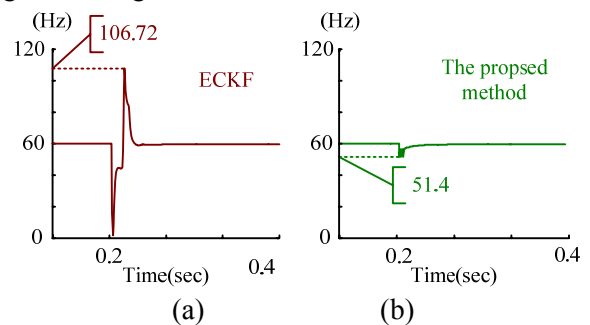


Fig.8 Frequency estimations for the test signal with condition 3 (a) The ECKF method (b) The proposed method

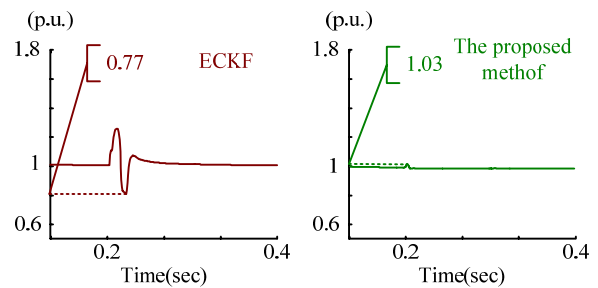


Fig.9 Amplitude estimations for the test signal with condition 3 (a) The ECKF method (b) The proposed method

**Case 2: Slow Change of Frequency:** In this simulation, the test signal of a sinusoidal wave has white noise with zero mean and a standard deviation of 0.01 p.u. The signal frequency decays from 60 Hz with a rate of 20 Hz/s to 59.5 Hz in the estimated period from 0.200 to 0.225 s, the variable formulation is as follows and its signal waveform is shown in Fig.10:

$$f = \begin{cases} 60 & \text{Hz,} & 0 \text{ sec} \leq t \leq 0.2\text{sec} \\ 64 - 20t & \text{Hz,} & 0.2 \text{ sec} \leq t \leq 0.225\text{sec} \\ 59.5 & \text{Hz,} & t \geq 0.225\text{sec} \end{cases} \quad (29)$$

The results of frequency and amplitude estimations using the ECKF and the proposed method for testing a slow change of frequency are shown in Figs. 11 and 12, respectively. As seen from Fig.11, the proposed method only takes 0.030 s to track the variation as frequency changes from 0.200 to 0.225 s, which is quicker than the ECKF method. In addition, the ECKF cannot track the varying signal as shown from Fig.12 after the 0.2 s. However, the proposed method can be used to track the varying signal and has less overshooting during variation of frequency. This means that the proposed method is still effective for a slow varying frequency of a signal.

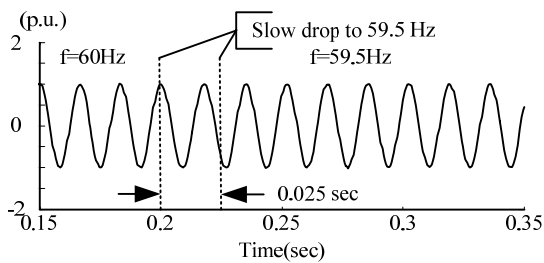


Fig.10 Sinusoidal signal with a slow change of frequency

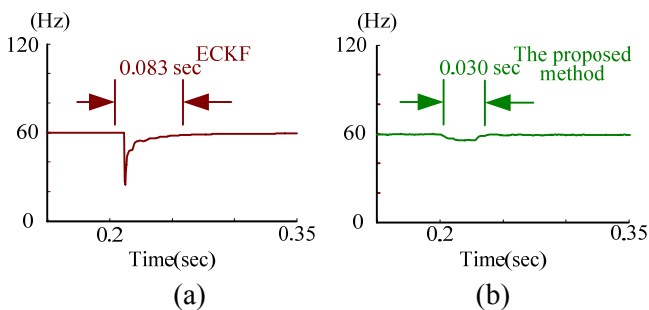


Fig.11 Frequency estimation of the signal as shown in Fig.10 (a) The ECKF method (b) The proposed method

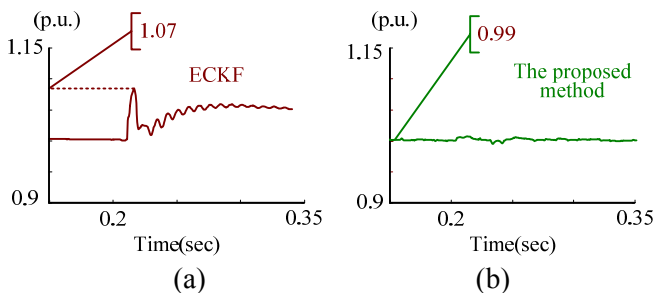


Fig.12 Amplitude estimation of the signal as shown in Fig.10 (a) The ECKF method (b) The proposed method

**Case 3: Signals Recorded from an Arc Furnace:**

A signal recorded from an arc furnace as shown in Fig.13 in a steel manufacturer factory is used in this case to check the feasibility of the proposed technique. As seen from Fig.14, the measured point is at the secondary of the main transformer 69/22.8 kV. The sampling frequency is 7.68 kHz and the recorded period is 25 s. For simplicity, Fig.13 only shows the voltage of phase c from 6.85 to 7.24 s with the arc furnace at the start of the melting process at time 7.00 s. The results of frequency estimation using the ECKF and the proposed methods as shown in Fig.15(a) are 1034 and 253 Hz at around 7.00 sec, respectively. Nevertheless, the results obtained from the ECKF method has little oscillations in the estimation. Similarly, the results of amplitude estimation using those methods are shown in Fig.15(b). As shown in Fig.15(b), oscillations have also occurred in the results of amplitude estimation using the ECKF method. However, the proposed method does not occur the phenomenon of oscillations in frequency and amplitude estimations. This means the proposed method is effective for a signal which is changed rapidly.

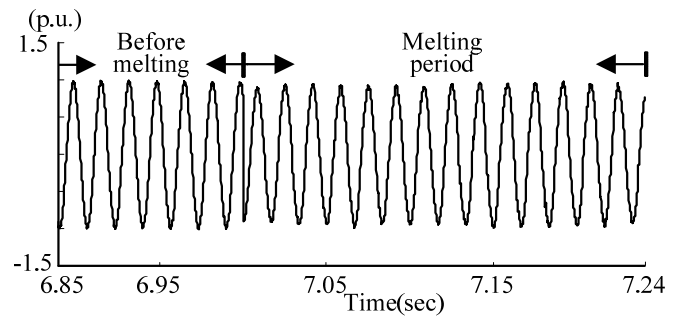


Fig.13 Voltage waveform of the phase c recorded from an arc furnace

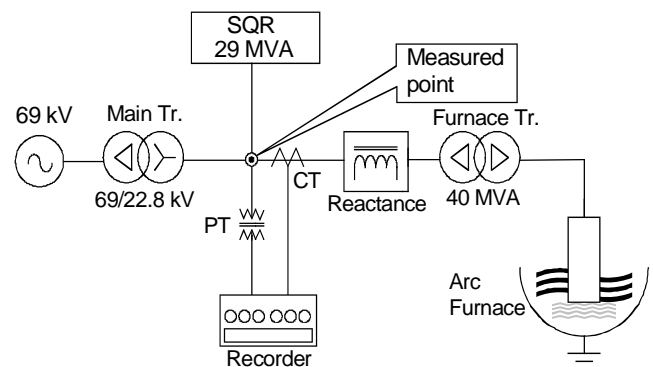


Fig.14 Single-line diagram for measuring an actual signal at a plant

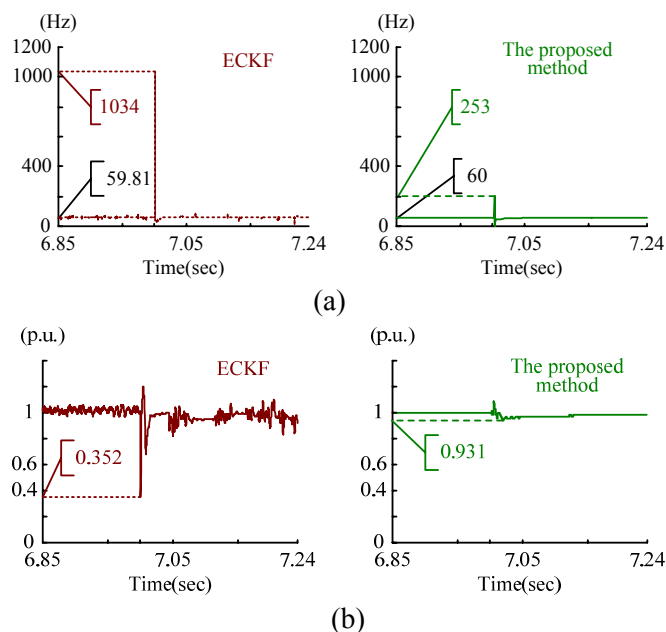


Fig.15 Frequency and amplitude estimations for the signal as shown in Fig.14 (a) Frequency estimations (b) Amplitude estimation

#### 4 Conclusion

This paper presents a method consisted of a robust extended complex Kalman filter and a sliding fuzzy controller (RECKF-SFC) for frequency and amplitude estimations of distorted signals in a power system. The proposed approach is based on applying the slide fuzzy controller to adjust the robust algorithm. A robust scheme is embedded into the ECKF algorithm to restrain the unusual measured value and enhance the estimated accuracy. As mentioned before, the results of frequency and amplitude estimations of distorted signals using the RECKF-SFC algorithm are better than the ECKF method. The RECKF-SFC not only can react to the change condition in real time for parameters tracking in a power system, but can also accurately estimate their values.

#### References

- [1] P. Kumar, S. C. Gupta, and B. Gupta, "Frequency deviation transducer for power system applications," *IEEE Transactions on Power Apparatus and Systems*, vol. PAS-94, no. 4, pp. 1270-1273, July/August 1975.
- [2] R. Aghazadeh, H. Lesani, M. Sanaye-Pasand, and B. Ganji, "New technique for frequency and amplitude estimation of power system signals," *IEE Proceedings-Generation, Transmission and Distribution*, vol.152, no.3, pp.435-440, May 2005.
- [3] A. G. Phadke, J. S. Thorp, and M. G. Adamlak, "A new measurement technique for tracking voltage phasors, local system frequency and rate of change of frequency," *IEEE Transactions on Power Apparatus and Systems*, vol. PAS-102, pp. 1025-1039, May 1983.
- [4] R. Yang and X. Hui, "A novel algorithm for accurate frequency measurement using transformed consecutive points of DFT," *IEEE Transactions on Power Systems*, vol.23, no.3, pp.1057-1062, August 2008.
- [5] T. Lobos and J. Rezmer, "Real-time determination of power system frequency," *IEEE Transactions on Instrumentation and Measurement*, vol. 46, no. 4, pp. 877-881, August 1997.
- [6] M. S. Sachdev and M. M. Giray, "A least square technique for determining power system frequency," *IEEE Transactions on Power Apparatus and Systems*, vol. PAS-104, pp. 427-443, May 1985.
- [7] A. K. Pradhan, a. toutray and A. Basak, "Power system frequency estimation using least mean square technique," *IEEE Transactions on Power Delivery*, vol. 20, no.3, pp. 1812-1816, July 2005.
- [8] P. J. Hargrave, "A tutorial introduction to Kalman filtering," *IEE Colloquium on Kalman Filter: Introduction, Application and Future Development*, pp.1-6, February 1989.
- [9] A. A. Girgis and W. L. Peterson, "Adaptive estimation of power system frequency deviation and its rate of change for calculating sudden power system overloads," *IEEE Transactions on Power Delivery*, vol. 5, no.2, pp. 585-594, April 1990.
- [10] H. M. Beides, G. T. Heydt, "Dynamic state estimation of power system harmonics using Kalman filter methodology," *IEEE Transactions on*, vol.6, pp.1663-1670, October 1991.
- [11] P. Tichavsky and A. Nehorai, "Comparative study of four adaptive frequency trackers," *IEEE Transactions on Signal Processing*, vol.45, pp.1473-1484, June 1997.
- [12] V. V.Terzija, N. B. Djuric, and B. D. Kovacevic, "Voltage phasor and local system frequency estimation using Newton type algorithm," *IEEE Transactions on Power Delivery*, vol. 9, no.3, pp. 1368-1374, July 1994.
- [13] V. V.Terzija, "Improved recursive Newton-type algorithm for power system relaying and measurement," *IEEE Transactions on Instrumentation and Measurement*, vol. 145, no. 1, pp. 877-881, January 1998.
- [14] J. Szafran and W. Rebizant, "Power System frequency estimation," *IEE Proceedings-*

- Generation, Transmission and Distribution*, vol.145, no.5, pp.578-582, September 1998.
- [15] T. S. Sidhu and M. S. Sachdev, "An iterative Technique for Fast and accurate measurement of power system frequency," *IEEE Transactions on Power Delivery*, vol. 13, no. 1, pp. 109-115, January 1998
- [16] A. Routray, A. K. Pradhan, and K. P. Rao, "A novel Kalman filter for frequency estimation of distorted signal in power systems," *IEEE Transactions on Instrumentation and Measurement*, vol.51, no.3, pp.469-479, June 2002.
- [17] K. Nishiyama, "A nonlinear filter for estimating a sinusoidal signal and its parameters in white noise: On the case of a single sinusoid," *IEEE Transactions on Signal Processing*, vol.45, no.4, pp.970-981, April 1997.
- [18] P. K. Dash, A. K. Pradhan, G. Panda, "Frequency estimation of distorted power system signals using extended complex Kalman filter," *IEEE Transactions on Power Delivery*, vol.14, no.3, pp761-766, July 1999.
- [19] P. K. Dash, R. K. Panda, G. Panda, "An extended complex Kalman filter for frequency measurement of distorted signals," *IEEE Transactions on Instrumentation and Measurement*, vol.49, no.4, pp.746-753, August 2000.
- [20] P. K. Dash and M. V. Chilukuri, "Hybrid S-transform and Kalman filtering approach for detection and measurement of short duration disturbances in power networks," *IEEE Transactions on Instrumentation and Measurement*, vol.53, no.2, pp.746-753, April 2004.
- [21] K. K. Yu, N. R. Watson, and J. Arrillaga, "An adaptive Kalman filter for dynamic harmonic state estimation and harmonic injection tracking," *IEEE Transactions on Power Delivery*, vol.20, no.2, pp.1577-1584, April 2006.
- [22] J. R. Macias, and A. G. Exposito, "Self-tuning of Kalman filters for harmonic computation," *IEEE Transactions on Power Delivery*, vol.21, no.1, pp.501-503, January 2006.
- [23] S. J. Huang and K. R. Shih, "Dynamic state-estimation scheme including nonlinear measurement-function considerations," *IEE Proceedings-Generation, Transmission and Distribution*, vol.149, no.6, pp.673-678, November 2002.
- [24] K. R. Shih and S. J. Huang, "Application of a robust algorithm for dynamic state estimation of a power system," *IEEE Transactions on Power Systems*, vol.17, no.1, pp.141-147, February 2002.
- [25] C. H. Huang, C. H. Lee, K. J. Shih, and Y. J. Wang, "Frequency estimation of distorted power system using a robust algorithm," *IEEE Transactions on Delivery*, vol.23, no.1, pp.41-51, January 2008.
- [26] J. M. Lin, S. J. Huang and K. R. Shih, "Application of sliding surface-enhanced fuzzy control for dynamic state estimation of a power system," *IEEE Transactions on Power Systems*, vol.18, no.2, pp.570-577, May 2003.
- [27] J. E. Slotine, "Sliding controller design for nonlinear system," *International Journal of Control*, vol. 40, pp. 421-434, 1984.